arXiv:2102.07262v1 [cond-mat.str-el] 14 Feb 2021

Destabilization of ferromagnetism by frustration and realization of a nonmagnetic Mott transition in the quarter-filled two-orbital Hubbard model

Katsunori Kubo
Advanced Science Research Center, Japan Atomic Energy Agency, Tokai, Ibaraki 319-1195, Japan
(Dated: January 4, 2022)

The two-orbital Hubbard model on a square lattice at quarter filling (electron number per site $n = 1$) is investigated by the variational Monte Carlo method. For the variational wave function, we include short-range doublon-holon binding factors. We find that the energy of this wave function is lower than that of the density-density Jastrow wave function partially including long-range correlations used in a previous study. We introduce frustration to the model by the next-nearest-neighbor hopping t' in addition to the nearest-neighbor hopping t. For $t' = 0$, a ferromagnetic state with staggered orbital order occurs by increasing the Coulomb interaction U before the Mott transition takes place. By increasing t', the region of this ferromagnetic phase shrinks, and the Mott transition without magnetic order occurs.

I. INTRODUCTION

The Mott transition is one of the most remarkable phenomena emerging from electron correlation. According to band theory, a system with an odd number of electrons per unit cell is a metal since at least one band is partially filled when we consider the spin degrees of freedom. However, there are insulators in which the electron number per unit cell is odd, e.g., MnO [1]. To explain these insulators, the importance of the Coulomb interaction between electrons was suggested by Mott and Peierls [2, 3] and insulators in which the electron correlation plays a crucial role for the realization of the insulating state are called Mott insulators.

To investigate the transition to the Mott insulator, the Mott transition, the single-orbital Hubbard model at half filling, i.e., electron number per site $n = 1$, is a typical model. When the onsite Coulomb interaction U is much smaller than the bandwidth W, the system should be in a metallic state. On the other hand, for $U \gg W$, most sites are occupied by a single electron and the electrons rarely move due to the large Coulomb interaction. Then, the system is expected to be insulating. Thus, the Mott transition should take place at $U \simeq W$. However, it is a hard task to describe the Mott transition theoretically since it is a many-body problem.

To describe the electron correlation, Gutzwiller proposed a variational wave function [the Gutzwiller wave function (GWF)] [4] and an approximation (the Gutzwiller approximation) [5] to evaluate physical quantities in the GWF. By applying the Gutzwiller approximation for $n = 1$, Brinkman and Rice pointed out that the system becomes insulating at a finite value of U [6]. The GWF for the single-orbital Hubbard model is given by $\prod_{\boldsymbol{r}}[1-(1-g)n_{\boldsymbol{r}\uparrow}n_{\boldsymbol{r}\downarrow}]|\Phi\rangle$, where $n_{\boldsymbol{r}\sigma}$ is the electron number operator of spin σ at site $\boldsymbol{r}$ and $|\Phi\rangle$ is the ground state wave function for $U = 0$. The Gutzwiller parameter g tunes the probability of double occupancy at each site. If $g = 0$, the double occupancy is completely prohibited and electrons cannot move at all; that is, the system is insulating. Brinkman and Rice found that g becomes zero at a finite U by employing the Gutzwiller approximation.

The complete suppression of double occupancy is an artifact of the approximation. As long as U is finite, while the frequency may be low, double occupancy should occur to reduce the kinetic energy. To avoid introducing approximations, the variational Monte Carlo (VMC) method was applied to the Hubbard model [7]. Then, a finite g was obtained even for a large U. Moreover, the Mott transition disappeared in the VMC calculation; that is, it was revealed that the GWF cannot describe the Mott transition at least in one- and two-dimensional lattices. The absence of the Mott transition in the GWF was also shown analytically for the one-dimensional case [8]. The reason can be understood as follows. In the GWF, when a pair of a doubly occupied site (doublon) and an empty site (holon) is created, the wave function is multiplied by the factor g. This factor does not change even when the distance between the doublon and holon increases (top panels in Fig. 1). In other words, the doublon and holon move freely after they are created. For $U < \infty$, the numbers of doublons and holons are finite and they can move freely; that is, the system is metallic, within the GWF. Thus, the GWF cannot describe the Mott insulating state.

Later, it became clear that inclusion of intersite correlations improves the situation [9, 10]. Here, we consider the wave function including the doublon-holon binding factors [doublon-holon binding wave function (DHWF)] [11, 12]. In the DHWF, the wave function is multiplied by additional factors when a doublon and a holon separate from nearest-neighboring sites (bottom panels of Fig. 1). It was shown that by an effect of these factors, the DHWF can describe the Mott transition [9].

Another important issue of the Mott transition is the competition with magnetism. In the single-orbital Hubbard model for $n = 1$ with only the nearest-neighbor hopping t, the ground state is expected to be the antiferromagnetically ordered state for $U > 0$ due to the perfect nesting of the Fermi surface. The unit cell contains two sites in the antiferromagnetic (AF) state; that is, there are two electrons per unit cell. Then, the AF state can be regarded as a band insulator. To realize the

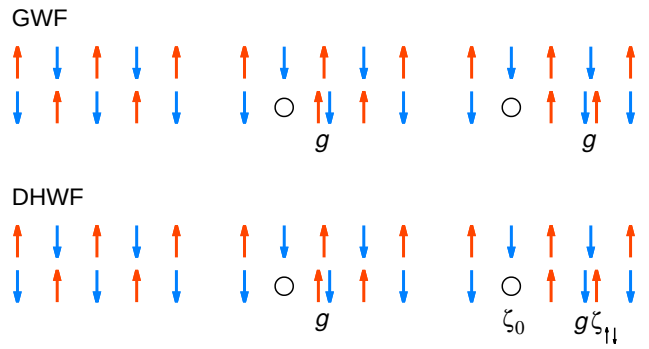


FIG. 1. Correlation factors for the GWF and DHWF. Here, we show them for the single-orbital model for simplicity. When a pair of a doublon and a holon is created, the factor g appears (middle panels). In the GWF, the doublon and holon move freely without a change in the factor (top right panel). In the DHWF, the factors ζ_0 and $\zeta_{\uparrow\downarrow}$ appear when the pair separates (bottom right panel), where 0 and $\uparrow\downarrow$ denote the holon and doublon states, respectively. In this figure, we have considered only the nearest-neighbor doublon-holon binding factors for clarity.

Mott insulating state without ambiguity, it is necessary to destabilize the antiferromagnetism. A plausible way is to introduce frustration [13–22]. For example, it is found that the region of the AF phase shrinks by increasing the next-nearest-neighbor hopping t', and the nonmagnetic Mott insulating phase appears [13, 17, 20, 21, 23].

In this paper, based on the above developments in the single-orbital model, we extend the research on the Mott transition to the two-orbital model. We apply the VMC method to the two-orbital Hubbard model by employing the DHWF. The interplay of the spin and orbital degrees of freedoms leads to intriguing phenomena such as orbital ordering and itinerant ferromagnetism, and many theoretical studies have been conducted using this model. To investigate the Mott transition, we consider integer values of n. For $n = 1$ without t', the ground state changes from the paramagnetic (PM) state to a ferromagnetic (FM) state with staggered orbital order by increasing the Coulomb interaction [24–34]. It was found that partially spin polarized states are hard to realize [28–31, 34], and in the following, we consider only the completely spin polarized state, in which only the majority spin states are occupied, as the FM state. For $n = 2$ without t', the ground state is the AF state without orbital order [28, 31, 34]. In both ordered phases, the electron number per unit cell is an even number, and these phases can be regarded as band insulating phases.

The Mott transition has also been investigated for the two-orbital and multiorbital Hubbard models [34–42] by assuming the PM phase. In these studies, the models with only the nearest-neighbor hopping are employed. Then, if we allow for magnetic states, the nonmagnetic Mott insulating phase disappears [34]. Thus, we need to introduce frustration.

In the case of $n = 2$, the magnetic phase to be destabilized to realize the nonmagnetic Mott transition is the AF phase, and the situation may be similar to the single-orbital model. In addition, the electron number per site is even, and the distinction between the band insulator and Mott insulator would be unclear. Thus, in this study, we concentrate on the case of quarter filling $n = 1$. If an insulating state appears in the PM phase for $n = 1$, it is a Mott insulator without ambiguity. We expect that by introducing frustration, we can destabilize the FM phase since this ferromagnetism is supported by the staggered ordering of the orbital degrees of freedom. Frustration usually destroys an AF state and the destabilization of the ferromagnetism by frustration is not so trivial and worth investigating.

II. MODEL AND WAVE FUNCTIONS

The two-orbital Hubbard model is given by

$$\begin{aligned} H = &\sum_{\boldsymbol{k},\tau,\sigma} \epsilon_{\boldsymbol{k}} c^\dagger_{\boldsymbol{k}\tau\sigma} c_{\boldsymbol{k}\tau\sigma} + U \sum_{\boldsymbol{r},\tau} n_{\boldsymbol{r}\tau\uparrow} n_{\boldsymbol{r}\tau\downarrow} \\ &+ U' \sum_{\boldsymbol{r}} n_{\boldsymbol{r}1} n_{\boldsymbol{r}2} + J \sum_{\boldsymbol{r},\sigma,\sigma'} c^\dagger_{\boldsymbol{r}1\sigma} c^\dagger_{\boldsymbol{r}2\sigma'} c_{\boldsymbol{r}1\sigma'} c_{\boldsymbol{r}2\sigma} \\ &+ J' \sum_{\boldsymbol{r},\tau\neq\tau'} c^\dagger_{\boldsymbol{r}\tau\uparrow} c^\dagger_{\boldsymbol{r}\tau\downarrow} c_{\boldsymbol{r}\tau'\downarrow} c_{\boldsymbol{r}\tau'\uparrow}, \end{aligned} \tag{1}$$

where $c^\dagger_{\boldsymbol{r}\tau\sigma}$ is the creation operator of the electron with orbital τ (= 1 or 2) and spin σ (=$\uparrow$ or $\downarrow$) at site $\boldsymbol{r}$, $n_{\boldsymbol{r}\tau\sigma} = c^\dagger_{\boldsymbol{r}\tau\sigma} c_{\boldsymbol{r}\tau\sigma}$, and $n_{\boldsymbol{r}\tau} = \sum_\sigma n_{\boldsymbol{r}\tau\sigma}$. $c^\dagger_{\boldsymbol{k}\tau\sigma}$ is the Fourier transform of $c^\dagger_{\boldsymbol{r}\tau\sigma}$. U and U' are intraorbital and interorbital Coulomb interactions, respectively. J is the Hund's rule coupling and J' denotes the pair-hopping interaction. We use the relations $U = U' + J + J'$ and $J = J'$, which hold in many orbitally degenerate systems [43].

We consider the nearest-neighbor hopping t and the next-nearest-neighbor hopping t' on a square lattice. Then, the kinetic energy is written as

$$\epsilon_{\boldsymbol{k}} = -2t(\cos k_x + \cos k_y) - 4t' \cos k_x \cos k_y, \tag{2}$$

where we have set the lattice constant as unity. We can assume $t > 0$ without loss of generality since the sign of t can be changed by the transformation $c_{\boldsymbol{r}\tau\sigma} \to e^{i\boldsymbol{Q}\cdot\boldsymbol{r}} c_{\boldsymbol{r}\tau\sigma}$ [$\boldsymbol{Q} = (\pi, \pi)$] without changing the other terms of the model. Then, the bandwidth is $W = 4t + 4\max(t, 2|t'|)$.

The sign of t' changes physical quantities in the PM phase except for the electron-hole symmetric case $n = 2$ [20]. Preliminary calculations on an 8×8 lattice for $n = 1$ indicate that the FM state is stable against $t' < 0$ in comparison with $t' > 0$. The completely spin-polarized FM state at $n = 1$ has electron-hole symmetry, and its energy does not depend on the sign of t'. On the other hand, the energy of the PM state depends on the sign. As inferred from the kinetic energy at $\boldsymbol{k} = (0, 0)$, $\epsilon_{\boldsymbol{k}=(0,0)} = -4t-4t'$, the energy for $t' > 0$ is lower than that for $t' < 0$ at least for a weak Coulomb interaction with $|t'| \ll t$ at

low electron filling. Thus, the PM solution may become advantageous for $t' > 0$. In the following, we consider only $t' \geq 0$ to destabilize the FM state.

Concerning the variational wave functions, we discuss three types: the GWF, the DHWF, and the wave function with the density-density Jastrow factor used in a previous study [34].

The GWF for the two-orbital model [30, 31, 35, 44–47] is given by

$$|\Psi_{\rm GWF}\rangle = P_G|\Phi\rangle, \tag{3}$$

where $|\Phi\rangle$ is a one-electron wave function which we will give below. The Gutzwiller projection operator is defined as

$$P_G = \prod_{\boldsymbol{r}\gamma} \left[1 - (1 - g_\gamma) P_{\boldsymbol{r}\gamma}\right], \tag{4}$$

where γ denotes one of the 16 onsite states, $P_{\boldsymbol{r}\gamma}$ is the projection operator onto state γ at site $\boldsymbol{r}$, and g_γ is a variational parameter. In the following, $\gamma = 0$ denotes the holon state, i.e., empty state. Since the overall factor to the wave function is arbitrary, we can omit one variational parameter. In addition, by using the conservation of the number of electrons for each spin and orbital and symmetry of the system, we can reduce the number of g_γ to be optimized to 5 in the PM state without ferro-orbital order. Note that similar consideration reduces the number of Gutzwiller parameters to one in the single-orbital Hubbard model. There are four on-site states in the single-orbital model, but one parameter can be omitted by considering the overall factor to the wave function, and two further parameters are omitted due to the conservation of the up- and down-spin electrons.

The DHWF is given by

$$|\Psi_{\rm DHWF}\rangle = \prod_{i=1}^{2} P_d^{(i)} P_h^{(i)} P_G |\Phi\rangle. \tag{5}$$

$P_d^{(1)}$ is defined as

$$P_d^{(1)} = \prod_{\boldsymbol{r}} \left[1 - (1 - \zeta_\gamma^{(1)}) P_{\boldsymbol{r}\gamma} \prod_{\boldsymbol{a}} (1 - P_{\boldsymbol{r}+\boldsymbol{a}0})\right], \tag{6}$$

where D denotes the set of doublon states, i.e., onsite states with two electrons, and $\boldsymbol{a}$ denotes the vectors connecting nearest-neighbor sites. $P_d^{(1)}$ gives the factor $\zeta_\gamma^{(1)}$ when site $\boldsymbol{r}$ is in the doublon state γ and there is no holon at nearest-neighbor sites $\boldsymbol{r} + \boldsymbol{a}$. Similarly, $P_h^{(1)}$ is defined as

$$P_h^{(1)} = \prod_{\boldsymbol{r}} \left[1 - (1 - \zeta_0^{(1)}) P_{\boldsymbol{r}0} \prod_{\boldsymbol{a}\,\gamma\in D} (1 - P_{\boldsymbol{r}+\boldsymbol{a}\gamma})\right]. \tag{7}$$

The factor $\zeta_0^{(1)}$ appears when a holon exists without a nearest-neighboring doublon. By considering symmetry, four $\zeta_\gamma^{(1)}$ are independent in the PM state without ferro-orbital order. In this study, we also consider the next-nearest-neighbor hopping, and we should include doublon-holon binding factors for the next-nearest-neighbor sites. They are represented by $P_d^{(2)}$ and $P_h^{(2)}$ and are defined similarly to $P_d^{(1)}$ and $P_h^{(1)}$, respectively, by regarding $\boldsymbol{a}$ as the vectors connecting next-nearest-neighbor sites and replacing (1) with (2) in Eqs. (6) and (7).

We will compare some of our results with a previous study using the density-density Jastrow wave function [34]:

$$|\Psi_{\rm Jastrow}\rangle = P_J|\Phi\rangle, \tag{8}$$

with

$$P_J = \exp\left(-\frac{1}{2}\sum_{\boldsymbol{r}\boldsymbol{r}'\tau\tau'} v_{\boldsymbol{r}\boldsymbol{r}'}^{\tau\tau'} n_{\boldsymbol{r}\tau} n_{\boldsymbol{r}'\tau'}\right). \tag{9}$$

There are only two parameters for any distance, $v_{\boldsymbol{r}\boldsymbol{r}'}^{11} = v_{\boldsymbol{r}\boldsymbol{r}'}^{22}$ and $v_{\boldsymbol{r}\boldsymbol{r}'}^{12} = v_{\boldsymbol{r}\boldsymbol{r}'}^{21}$, unless we consider ferro-orbital order. However, this Jastrow wave function partially includes the long-range correlations. On the other hand, the GWF and DHWF include only short-range correlations but carefully treat them.

Without orbital order, the one-electron part of the wave function $|\Phi\rangle$ is constructed by filling electrons inside the Fermi surface defined by $\epsilon_{\boldsymbol{k}}$. For an antiferro-orbital ordered state with ordering vector $\boldsymbol{Q} = (\pi, \pi)$, we consider an effective Hamiltonian:

$$H_{\boldsymbol{k}\tau} = \begin{pmatrix} \epsilon_{\boldsymbol{k}} & -\Delta_\tau \\ -\Delta_\tau & \epsilon_{\boldsymbol{k}+\boldsymbol{Q}} \end{pmatrix}, \tag{10}$$

where $\Delta_\tau = \Delta_o(\delta_{\tau 1} - \delta_{\tau 2})$. We construct $|\Phi\rangle$ by filling electrons from the bottom of the energy of this effective Hamiltonian. Δ_o is a variational parameter. $|\Phi\rangle$ is reduced to that without orbital order for $\Delta_o = 0$. As mentioned in the Introduction, at least for $t' = 0$, it is difficult to realize a partially spin polarized FM state [28–31, 34]. Thus, we consider only the majority-spin electrons in the FM state.

We optimize the variational parameters in each wave function to reduce the expectation value of the energy evaluated by the Monte Carlo method. Physical quantities are also calculated by the Monte Carlo method for the variational wave functions with the optimized variational parameters.

III. RESULTS

In the following, we show the calculated results for an $L \times L$ square lattice of $L = 12$ with antiperiodic-periodic boundary conditions. To examine the finite-size effect, we also show some results for $L = 10$ and 14. The number of electrons per site is fixed as $n = 1$, i.e., quarter-filling. We have searched for the antiferro-orbital order in the PM phase but we could not find it. Thus, we show results only for the PM state without orbital order and the FM

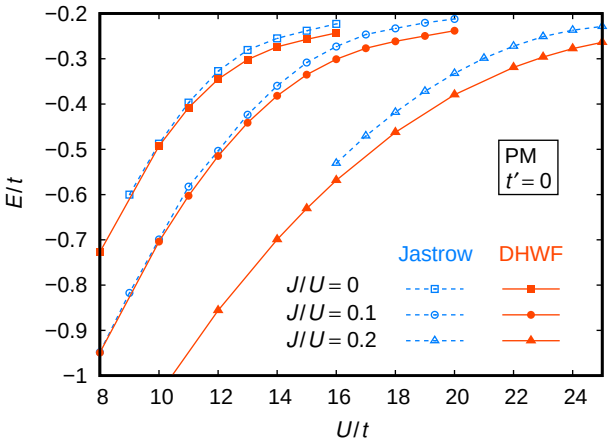


FIG. 2. Energy E per site as a function of U for the Jastrow wave function (Ref. [34], open symbols) and for the DHWF (solid symbols) for the Hund's rule coupling $J = 0$ (squares), $J = 0.1U$ (circles), and $J = 0.2U$ (triangles). The next-nearest-neighbor hopping t' is set to zero.

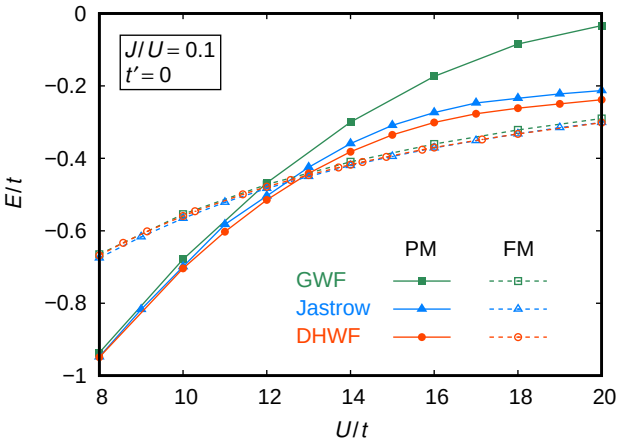


FIG. 3. Energy E per site as a function of U in the PM (solid symbols) and FM (open symbols) states of the GWF (squares), of the Jastrow wave function (Ref. [34], triangles), and of the DHWF (circles) for $J = 0.1U$. The next-nearest-neighbor hopping t' is set to zero.

state with antiferro-orbital order in the following. Some results for $t' = 0$ are compared with a previous study using the density-density Jastrow wave function [34] for the same lattice size with the same boundary conditions.

First, we compare the energy of the PM state for $t' = 0$ in the Jastrow wave function [34] and the DHWF (Fig. 2). The energy of the DHWF is lower than that of the Jastrow wave function in the entire range. The lower energy indicates that the careful treatment of the short-range correlations is more important than the partial inclusion of the long-range correlations, at least for $n = 1$. In addition, the DHWF includes the spin-dependent correlations; for example, doublons with parallel and antiparallel spin configurations correspond to different variational parameters. On the other hand, the density-density Jastrow wave function does not include such spin dependence, and the energy difference between these wave functions becomes larger as the Hund's rule coupling J increases.

Figure 3 shows the energy of the PM state without orbital order and of the FM state with antiferro-orbital order for the three kinds of wave functions for $J = 0.1U$. For the PM state, the GWF has much higher energy than those of the Jastrow wave function and DHWF. That is, the inclusion of the intersite correlations brings a marked improvement in the PM state. Between the wave functions with the intersite correlations, as already mentioned above, the DHWF has lower energy than the Jastrow wave function. For the FM state, the values of energy of these three wave functions are very close. This closeness means that the intersite correlations are not very important for the ordered phase in comparison with the PM phase. For a large U, $U \gtrsim 16t$, the GWF has slightly higher energy than the other wave functions. For a smaller U, $U \lesssim 10t$, the Jastrow wave function has slightly lower energy than the other wave functions. For a smaller-U case, since electrons can move easily in comparison with a larger-U case, the long-range correlations play roles, and the Jastrow wave function has an advantage. We determine the FM transition point $U_{\rm FM}$ by comparing the energy of the PM and FM states. For $J = 0.1U$ with $t' = 0$, the FM transition occurs at $U_{\rm FM} \simeq 13t$ in the DHWF. In the Jastrow wave function, $U_{\rm FM}/t = 12.5 \pm 0.5$ was reported [34]. Since the values of energy for the DHWF and the Jastrow wave function are close around the transition point, these wave functions give close values of $U_{\rm FM}$.

In the rest of this section, we show the results obtained with the DHWF.

To examine the finite-size effect, we show the energy of PM and FM states for $L = 10$, 12, and 14 as a function of U for $J = 0.1U$ in Fig. 4. The finite-size effect on energy is very weak and as a result, the size dependence of $U_{\rm FM}$ is weak.

Figure 5 shows the momentum distribution function $n(\boldsymbol{k}) = \langle c^\dagger_{\boldsymbol{k}\tau\sigma} c_{\boldsymbol{k}\tau\sigma} \rangle$ for $U = 12t$, $J = 0$, and $t' = 0$ in the PM phase, where $\langle \cdots \rangle$ denotes the expectation value in the optimized wave function. This quantity does not depend on the orbital and spin in the PM phase. Due to the correlation effect, the jump at the Fermi momentum is reduced from unity. We define the renormalization factor Z by this jump along (π, π)–$(0, 0)$. Z is inversely proportional to the effective mass, and in an insulating state $Z = 0$. To estimate Z in a finite-size lattice, we extrapolate $n(\boldsymbol{k})$ from above and below the Fermi momentum, as shown in Fig. 5.

In Fig. 6, we show the U dependence of Z for $t' = 0$ and $J = 0$ in the PM phase. Z is reduced from unity by increasing U and seems to vanish at $U \simeq 14t$. From the evaluation procedure of Z, it is difficult to determine Z accurately for a finite-size lattice when Z is small. The number of data points available to determine Z is $O(L)$

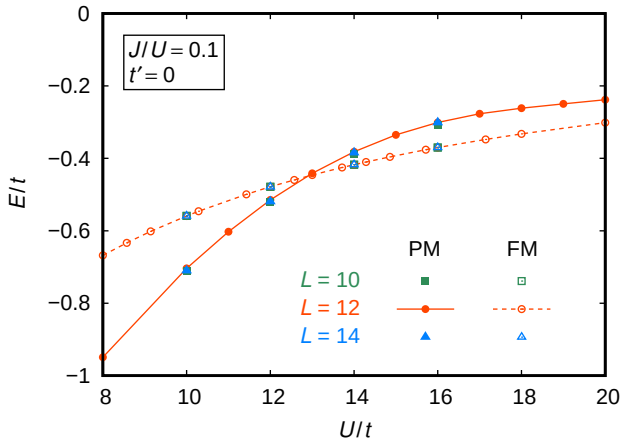


FIG. 4. Energy E per site as a function of U in the PM (solid symbols) and FM (open symbols) states for $L = 10$ (squares), for $L = 12$ (circles), and for $L = 14$ (triangles) for $J = 0.1U$. The next-nearest-neighbor hopping t' is set to zero.

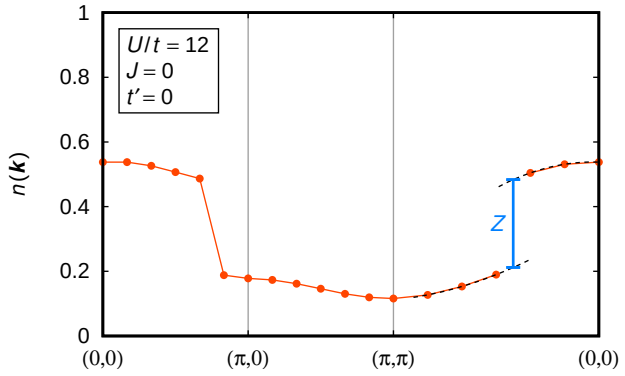


FIG. 5. Momentum distribution function $n(\boldsymbol{k}) = \langle c^{\dagger}_{\boldsymbol{k}\tau\sigma} c_{\boldsymbol{k}\tau\sigma} \rangle$ for $U = 12t$, $J = 0$, and $t' = 0$ in the PM phase. The renormalization factor Z is estimated by extrapolating $n(\boldsymbol{k})$ from above and below the Fermi momentum along (π, π)–$(0, 0)$ (dashed lines). Due to the antiperiodic boundary condition for the x direction, we shift k_x by π/L ($L = 12$); for example, (π, π) denoted in this figure actually means the point $(\pi - \pi/L, \pi)$.

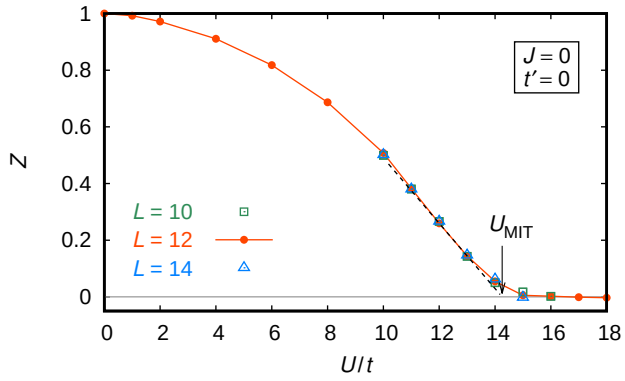


FIG. 6. Renormalization factor Z as a function of U for $J = 0$ and $t' = 0$ in the PM phase for $L = 10$ (squares), for $L = 12$ (circles), and for $L = 14$ (triangles). Here, we estimate $U_{\rm MIT}$ by linearly extrapolating Z to zero from data of $Z > 0.1$ for $L = 12$.

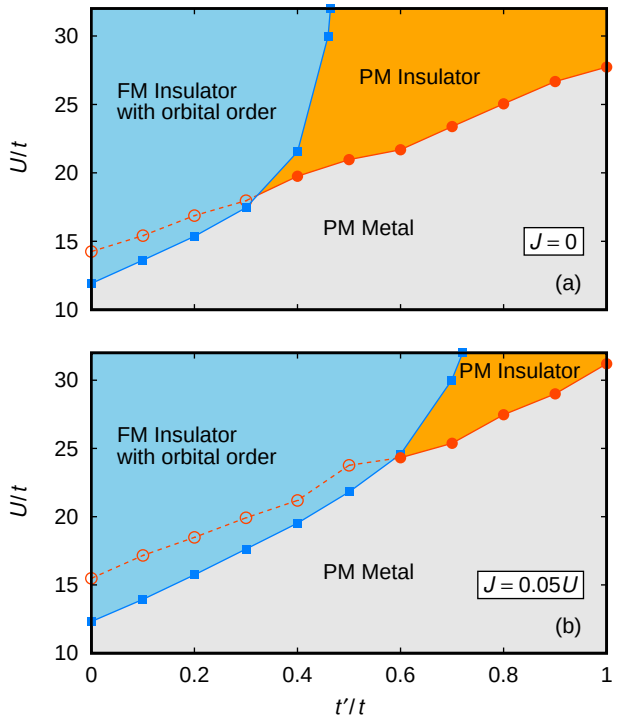


FIG. 7. Phase diagrams for the two-orbital Hubbard model with the next-nearest-neighbor hopping t' (a) for $J = 0$ and (b) for $J = 0.05U$. The open circles with the dashed lines indicate the metal-insulator transition in the PM phase when we ignore the FM state.

for an $L \times L$ lattice, and it may be difficult to determine Z smaller than $1/L$. Indeed, we observe the size dependence of Z for $U \simeq 14t$. Thus, here, we determine the metal-insulator transition point $U_{\rm MIT}$ by linearly extrapolating data with $Z > 0.1$ to $Z = 0$ as shown in Fig. 6. By using different initial variational parameters, we estimate errors in Z as $\delta Z \lesssim 0.01$ for $Z \simeq 0.1$ in the present calculation. Then, the error in $U_{\rm MIT}$ due to the extrapolation is estimated to be $\delta U_{\rm MIT} \lesssim 0.1t$. Note that the error from the finite-size effect would be larger. To evaluate the value of $U_{\rm MIT}$ more accurately, we should carefully check the lattice-size dependence by using larger lattices. It is outside the scope of this study. In the density-density Jastrow wave function, the transition point was estimated as $U_{\rm MIT}/t = 13 \pm 1$ [34].

By determining $U_{\rm FM}$ and $U_{\rm MIT}$ for each t', we construct phase diagrams. For $J = 0$ [Fig. 7(a)], we obtain $U_{\rm MIT} \simeq 14t$ for $t' = 0$ in the PM phase (see Fig. 6), but the PM-FM transition already occurs at $U_{\rm FM} \simeq 12t$. Thus, the nonmagnetic Mott transition does not occur for $t' = 0$. By increasing frustration t', the staggered order

of the orbital would be destabilized. Indeed, we find that the FM insulating phase with orbital order shrinks, and the nonmagnetic Mott transition emerges at $t' \gtrsim 0.3t$. For $J = 0.05U$ [Fig. 7(b)], the phase diagram is similar to that for $J = 0$ at $t' \lesssim 0.3t$. By an effect of the Hund's rule coupling, which is expected to stabilize magnetic phases, the region of the FM phase is extended, in particular, for $t' \gtrsim 0.3t$.

For $J = 0$, antiferro-orbital order without ferromagnetism may be expected, but we could not find such a phase. Instead, we found the FM state with antiferro-orbital order even for $J = 0$. In this state, each orbital state is ferromagnetic due to the strong correlation effect within each orbital. Note that this result does not mean the realization of a FM state in the single-orbital Hubbard model for $n = 0.5$. The realization of the ferromagnetism in the two-orbital Hubbard model is supported by the antiferro-orbital order. For $J = 0$, this FM state is equivalent to an antiferro-orbital ordered state in which the $\tau = 1$ orbital states are occupied with only up-spin electrons and the $\tau = 2$ orbital states are occupied with only down-spin electrons. For a finite J, this state should have higher energy than the FM state.

IV. SUMMARY

We have investigated the quarter-filled two-orbital Hubbard model on a square lattice with next-nearest-neighbor hopping t' using the VMC method.

In the variational wave function DHWF, we have considered the nearest-neighbor and next-nearest-neighbor doublon-holon binding factors. We have found that the energy for the PM state of the DHWF is lower than that of the density-density Jastrow wave function used in a previous study [34]. This result means that a careful treatment of the short-range correlations is more important than partial inclusion of the long-range correlations, at least for $n = 1$.

In the ordinary two-orbital Hubbard model with the only nearest-neighbor hopping t, the FM transition with staggered orbital order occurs before the Mott transition when we increase the Coulomb interaction U. To realize the nonmagnetic Mott transition, it is necessary to suppress the FM phase. For this purpose, we have introduced frustration to the model by the next-nearest-neighbor hopping t', which is expected to destabilize the staggered orbital order supporting the FM state. We have found that the region of the FM phase is, indeed, shrunk by t' and the nonmagnetic Mott transition occurs. Thus, it is revealed that the realization of the nonmagnetic Mott transition is not limited to the simple single-orbital case and the research field of Mott physics can be extended to multiorbital systems.

We also searched for the antiferro-orbital order in the PM phase, but we could not find it, while it was reported when using a dynamical mean-field theory [33]. It is interesting to realize such a pure orbital order by improving the model and/or the wave function for a finite-dimensional lattice. In particular, if such a phase were to appear between the PM insulator (Mott insulator) and the FM insulator with orbital order, the microscopic description of successive transitions between these phases would be intriguing. This phase is an important future problem.

[1] J. H. de Boer and E. J. W. Verwey, Semi-conductors with partially and with completely filled $3d$-lattice bands, Proc. Phys. Soc. **49**, 59 (1937).

[2] N. F. Mott and R. Peierls, Discussion of the paper by de Boer and Verwey, Proc. Phys. Soc. **49**, 72 (1937).

[3] N. F. Mott, The Basis of the Electron Theory of Metals, with Special Reference to the Transition Metals, Proc. Phys. Soc. A **62**, 416 (1949).

[4] M. C. Gutzwiller, Effect of Correlation on the Ferromagnetism of Transition Metals, Phys. Rev. Lett. **10**, 159 (1963).

[5] M. C. Gutzwiller, Correlation of Electrons in a Narrow s Band, Phys. Rev. **137**, A1726 (1965).

[6] W. F. Brinkman and T. M. Rice, Application of Gutzwiller's Variational Method to the Metal-Insulator Transition, Phys. Rev. B **2**, 4302 (1970).

[7] H. Yokoyama and H. Shiba, Variational Monte-Carlo Studies of Hubbard Model. I, J. Phys. Soc. Jpn. **56**, 1490 (1987).

[8] W. Metzner and D. Vollhardt, Analytic calculation of ground-state properties of correlated fermions with the Gutzwiller wave function, Phys. Rev. B **37**, 7382 (1988).

[9] H. Yokoyama, Variational Monte Carlo Studies of Attractive Hubbard Model. I, Prog. Theor. Phys. **108**, 59 (2002).

[10] M. Capello, F. Becca, S. Yunoki, and S. Sorella, Unconventional metal-insulator transition in two dimensions, Phys. Rev. B **73**, 245116 (2006).

[11] T. A. Kaplan, P. Horsch, and P. Fulde, Close Relation between Localized-Electron Magnetism and the Paramagnetic Wave Function of Completely Itinerant Electrons, Phys. Rev. Lett. **49**, 889 (1982).

[12] H. Yokoyama and H. Shiba, Variational Monte-Carlo Studies of Hubbard Model. III. Intersite Correlation Effects, J. Phys. Soc. Jpn. **59**, 3669 (1990).

[13] T. Kashima and M. Imada, Magnetic and Metal–Insulator Transitions through Bandwidth Control in Two-Dimensional Hubbard Models with Nearest and Next-Nearest Neighbor Transfers, J. Phys. Soc. Jpn. **70**, 3052 (2001).

[14] H. Morita, S. Watanabe, and M. Imada, Nonmagnetic Insulating States near the Mott Transitions on Lattices with Geometrical Frustration and Implications for κ-$(ET)_2Cu_2(CN)_3$, J. Phys. Soc. Jpn. **71**, 2109 (2002).

[15] O. Parcollet, G. Biroli, and G. Kotliar, Cluster Dynamical Mean Field Analysis of the Mott Transition, Phys.

Rev. Lett. **92**, 226402 (2004).
[16] T. Watanabe, H. Yokoyama, Y. Tanaka, and J.-i. Inoue, Superconductivity and a Mott Transition in a Hubbard Model on an Anisotropic Triangular Lattice, J. Phys. Soc. Jpn. **75**, 074707 (2006).
[17] T. Mizusaki and M. Imada, Gapless quantum spin liquid, stripe, and antiferromagnetic phases in frustrated Hubbard models in two dimensions, Phys. Rev. B **74**, 014421 (2006).
[18] P. Sahebsara and D. Sénéchal, Antiferromagnetism and Superconductivity in Layered Organic Conductors: Variational Cluster Approach, Phys. Rev. Lett. **97**, 257004 (2006).
[19] B. Kyung and A. M. S. Tremblay, Mott Transition, Antiferromagnetism, and d-Wave Superconductivity in Two-Dimensional Organic Conductors, Phys. Rev. Lett. **97**, 046402 (2006).
[20] H. Yokoyama, M. Ogata, and Y. Tanaka, Mott Transitions and d-Wave Superconductivity in Half-Filled-Band Hubbard Model on Square Lattice with Geometric Frustration, J. Phys. Soc. Jpn. **75**, 114706 (2006).
[21] S. Onari, H. Yokoyama, and Y. Tanaka, Phase diagram of half-filled square lattice for frustrated Hubbard model, Physica C **463-465**, 120 (2007).
[22] R. T. Clay, H. Li, and S. Mazumdar, Absence of Superconductivity in the Half-Filled Band Hubbard Model on the Anisotropic Triangular Lattice, Phys. Rev. Lett. **101**, 166403 (2008).
[23] A. Yamada, K. Seki, R. Eder, and Y. Ohta, Magnetic properties and Mott transition in the square-lattice Hubbard model with frustration, Phys. Rev. B **88**, 075114 (2013).
[24] L. M. Roth, Simple Narrow-Band Model of Ferromagnetism Due to Intra-Atomic Exchange, Phys. Rev. **149**, 306 (1966).
[25] K. I. Kugel and D. I. Khomskii, Superexchange ordering of degenerate orbitals and magnetic structure of dielectric with Jahn-Teller ions, JETP Lett. **15**, 446 (1972).
[26] K. Kusakabe and H. Aoki, Magnetism in Two-Band Systems with Electron Correlation, Mol. Cryst. Liq. Cryst. **233**, 431 (1993).
[27] K. Kusakabe and H. Aoki, Metallic Ferromagnetism in the Two-Band Hubbard Model, Physica B **194-196**, 217 (1994).
[28] T. Momoi and K. Kubo, Ferromagnetism in the Hubbard model with orbital degeneracy in infinite dimensions, Phys. Rev. B **58**, R567 (1998).
[29] H. Sakamoto, T. Momoi, and K. Kubo, Ferromagnetism in the one-dimensional Hubbard model with orbital degeneracy: From low to high electron density, Phys. Rev. B **65**, 224403 (2002).
[30] K. Kubo, Ferromagnetism and orbital order in the two-orbital Hubbard model, J. Phys.: Conf. Ser. **150**, 042101 (2009).
[31] K. Kubo, Variational Monte Carlo study of ferromagnetism in the two-orbital Hubbard model on a square lattice, Phys. Rev. B **79**, 020407(R) (2009).
[32] R. Peters and T. Pruschke, Orbital and magnetic order in the two-orbital Hubbard model, Phys. Rev. B **81**, 035112 (2010).
[33] R. Peters, N. Kawakami, and T. Pruschke, Orbital order, metal-insulator transition, and magnetoresistance effect in the two-orbital Hubbard model, Phys. Rev. B **83**, 125110 (2011).
[34] C. De Franco, L. F. Tocchio, and F. Becca, Metal-insulator transitions, superconductivity, and magnetism in the two-band Hubbard model, Phys. Rev. B **98**, 075117 (2018).
[35] J. Bünemann, W. Weber, and F. Gebhard, Multiband Gutzwiller wave functions for general on-site interactions, Phys. Rev. B **57**, 6896 (1998).
[36] J. E. Han, M. Jarrell, and D. L. Cox, Multiorbital Hubbard model in infinite dimensions: Quantum Monte Carlo calculation, Phys. Rev. B **58**, R4199 (1998).
[37] Y. Ōno, M. Potthoff, and R. Bulla, Mott transitions in correlated electron systems with orbital degrees of freedom, Phys. Rev. B **67**, 035119 (2003).
[38] A. Koga, N. Kawakami, H. Yokoyama, and K. Kobayashi, Variational Monte Carlo Study of Two Dimensional Multi-Orbital Hubbard Model, AIP Conf. Proc. **850**, 1458 (2006).
[39] L. de' Medici, Hund's coupling and its key role in tuning multiorbital correlations, Phys. Rev. B **83**, 205112 (2011).
[40] L. de' Medici, J. Mravlje, and A. Georges, Janus-Faced Influence of Hund's Rule Coupling in Strongly Correlated Materials, Phys. Rev. Lett. **107**, 256401 (2011).
[41] Y. Takenaka and N. Kawakami, Variational Monte Carlo Study of Two-Dimensional Multi-Orbital Hubbard Model on Square Lattice, J. Phys.: Conf. Ser. **400**, 032099 (2012).
[42] J. I. Facio, V. Vildosola, D. J. García, and P. S. Cornaglia, On the nature of the Mott transition in multiorbital systems, Phys. Rev. B **95**, 085119 (2017).
[43] H. Tang, M. Plihal, and D. L. Mills, Theory of the spin dynamics of bulk Fe and ultrathin Fe(1 0 0) films, J. Magn. Magn. Mater. **187**, 23 (1998).
[44] T. Okabe, Generalization of Gutzwiller Approximation, J. Phys. Soc. Jpn. **66**, 2129 (1997).
[45] K. Kobayashi and H. Yokoyama, Stability of the superconducting state in the two-band Hubbard model on a triangular lattice, Physica C **445-448**, 162 (2006).
[46] K. Kubo and P. Thalmeier, Correlation Effects on Antiferromagnetism in Fe Pnictides, J. Phys. Soc. Jpn. **80**, SA121 (2011).
[47] K. Kubo and H. Onishi, Variational Wavefunction for the Periodic Anderson Model with Onsite Correlation Factors, J. Phys. Soc. Jpn. **86**, 013701 (2017).